ACS OMEGA

http://pubs.acs.org/journal/acsodf

Article

Cyclometallated Platinum(II) Complexes with Small Crown Ether Rings: Appropriate Choice of the Bridging Diphosphane to Coordinate Potassium Cations

Fátima Lucio-Martínez,* Francisco Reigosa, Brais Bermúdez, Harry Adams, M. Teresa Pereira, and José M. Vila*

Cite This: *ACS Omega* 2022, 7, 37256−37263

Read Online

ACCESS | Metrics & More | Article Recommendations | Supporting Information

ABSTRACT: This account reports the synthesis and structural characterization of the first cyclometallated platinum(II) complex that coordinates a potassium cation in a sandwich arrangement via two 15-crown-5 ether rings within the same molecule. The cooperation of the two small crown ether moieties allows the entrapment of the non-ideal potassium ion. The reaction of the parent thiosemicarbazone ligand 3,4-$(C_8H_{16}O_5)C_6H_3C(Me)$=NN−(H)C(=S)NHMe, **1**, containing the crown ether ring, with $K_2[PtCl_4]$, or alternatively with $PtCl_2(DMSO)_2$, and subsequent treatment with the diphosphanes $Ph_2PCH_2PPh_2$ (dppm) and $Ph_2PC(=CH_2)PPh_2$ (vdpp) produced the double nuclear platinacycles **3a**, **3b**, and **4**, probably via formation of the **2a** and **2b** intermediates. Complex **3a** with the K^+ cation in a sandwich coordination was slightly mixed with **3b** lacking any K^+. Alternatively, reaction of 1 with $K_2[PtCl_4]$ or with $PtCl_2(DMSO)_2$ followed by the diphosphane $Ph_2PC(=CH_2)PPh_2$ (vdpp) only gave the dinuclear phosphane-bridged compound **4**; this highlights the importance of choosing the right diphosphane ligand. Density functional theory calculations (B3LYP-D3/LANL2DZ-ECP-6.311++G**) revealed similar affinities for both dppm and vdpp derivatives to coordinate potassium cations. Crystal structure analysis was performed for compounds **3a** and **4**.

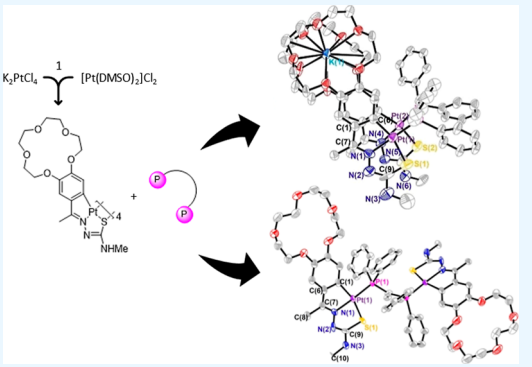

INTRODUCTION

Crown ethers are widely known neutral ligands which are quite adequate for entrapping metal cations. The corresponding complexes appear mainly in two conformations: a sole crown ligand surrounding the cation in its equatorial plane, in a crown style, or via the combination of two crown ligands coordinating the metal cation from above and below, in a sandwich style. In the former case, the coordination is size-selective, while in the latter one, coordination of cations too large to fit in the crown gap is possible. In both cases, an increase in the solubility in the desired solvent of the targeted cation is achieved. Crown ether complexes are usually fairly stable, and crown ethers are used either alone or as part of more complex structures, with applications in cation recognition,[1−3] in the extraction of metals,[4] for phase-transfer catalysis[5] in biomedical applications,[6,7] or luminescent materials[8] among others. In particular, the use of crown ethers for coordinating cations provides the driving force for the formation of gels,[9] to enhance their metal recognition capability[10,11] or for "pre-organizing" in the Diels−Alder reaction.[12] On the other hand, it is well known that cyclometallated moieties are robust scaffolds usually bench stable with a variety of applications, with one of the most frequent being the usage as catalytic precursors.[13−16]

It was in the beginning of the 21st century when Bezsoudnova[17] reported the first cyclometallated species bearing a crown ether moiety, and since then, extensive work in this field has been carried out trying to achieve compounds with the ether donor in the crown style for the development of potential sensors.[18−21] Then, in 2017, we described the first cyclometallated palladium(II) complex bearing two crown ether rings capable of coordinating a potassium cation in a sandwich style, and after detailed evaluation of the process confirmed by the single-crystal X-ray structure, we could conclude that the formation of the sandwich complex was favored by the possible pseudo $\pi-\pi$ interactions of the cyclometallated moieties.[22] For the 15-crown-5 ether, a sandwiched-type geometry has been suggested for complexation of the potassium cation by two 15-crown-5 ether moieties;[23] references may be found related to this sort of

Received: June 6, 2022
Accepted: September 14, 2022
Published: October 14, 2022

Scheme 1. (i) $K_2[PtCl_4]$ in $EtOH/H_2O$ and (ii) $[Pt(DMSO)_2Cl_2]$, MeOH

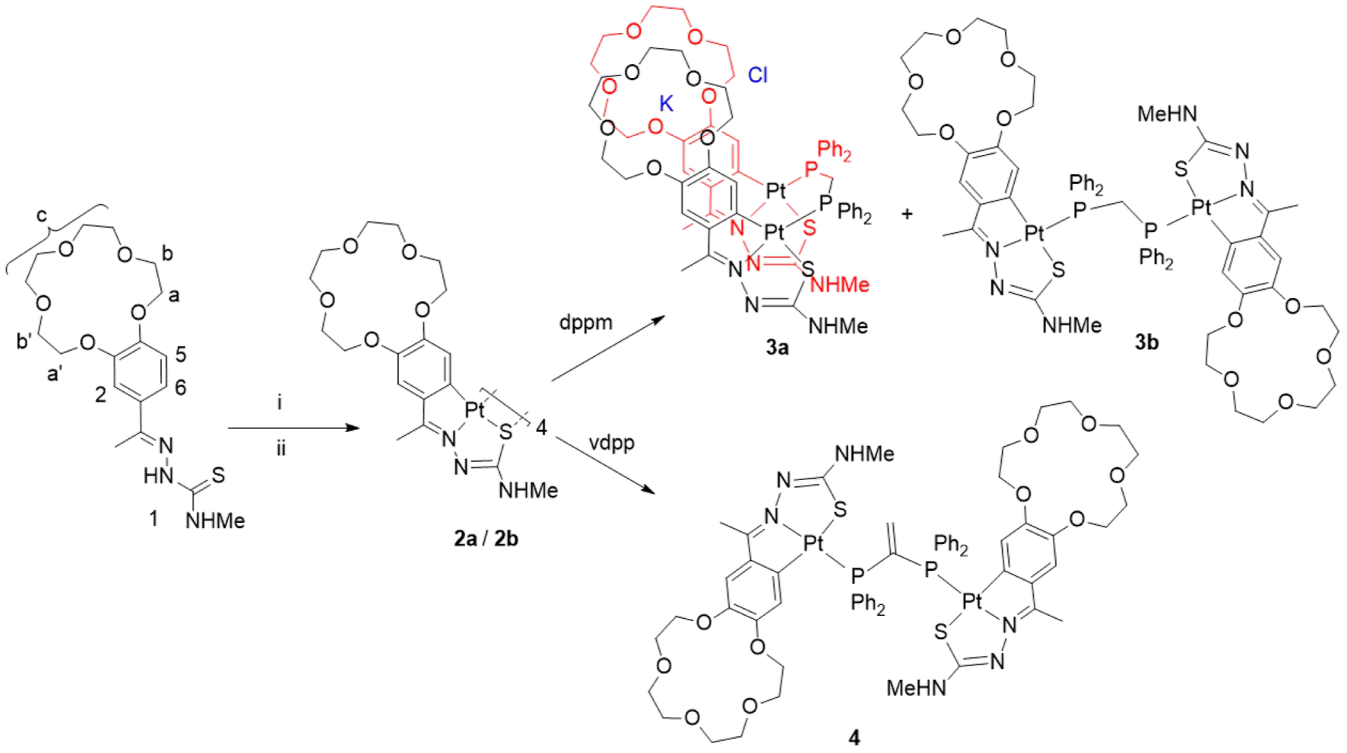

arrangement. Then, the crown ether may serve as an entrapping agent for K^+;[24] to sustain K^+ as the counterion;[25−27] and for making bis-sandwiched tetracrown complexes.[28]

Our next approach was (a) to check on the reproducibility of the reaction on metallacycles other than those with palladium(II), for which platinum(II) was the alternative choice; (b) to elucidate the mechanism of the formation of the sandwich structure, by means of density functional theory (DFT) calculations; (c) to study the influence of the bridging ligand linking the two cyclometallated moieties, for which two short-bite diphosphanes, dppm and vdpp, were considered. Herein, we report the results of these considerations with the preparation of the first cyclometallated platinum(II) complex that coordinates a potassium cation in a sandwich arrangement via two 15-crown-5 ether rings within the same molecule, fully corroborated by the crystal structure analysis for the platinacycle compound **3a**, as well as by the corresponding theoretical calculations.

RESULTS AND DISCUSSION

It is well known that the cyclometallation of thiosemicarbazones gives rise to the formation of tetranuclear complexes,[16,22,29−34] where the core of the structure consists of an eight-membered ring of alternating metal and sulfur atoms. In the case of thiosemicarbazone ligands with crown ether rings, one might assume that the crown rings should be able to adopt an arrangement capable of entrapping metal cations of the appropriate size. However, although the metallated rings are nearly parallel, they point out in quite opposite directions[35,36] and as a consequence of this structural disposition, the crown ether substituents on these rings are also oriented in different directions, far from the needed sandwich mode. Thus, hindering the possibility of enclosing metal cations, the rigidity of the molecule imposed by the central Pd_4S_4 ring impedes any approximation of the oxygen donors.[37] With this in mind, we considered it a challenging quest to study the coordination ability of these systems in the case of platinum(II) focusing on the dinuclear derivatives, as well as on the preference for the proper short-bite diphosphane ligand to bring the ether rings close together. Thus, reaction of a suspension of $K_2[PtCl_4]$ in ethanol with the ligand **1**, 3,4-$(C_8H_{16}O_5)C_6H_3C(Me)$=N−N(H)C(=S)NHMe, via i, gave a highly insoluble brown solid **2a**. In a similar manner, treatment of ligand **1** with $PtCl_2(DMSO)_2$, via ii, avoiding the presence of the potassium cation gave, after work-up, an orange solid **2b**. The compounds were too insoluble for NMR determination and were immediately used without further purification. Nevertheless, the IR spectra for both showed absence of the $\upsilon(N-H)_{hydrazinic}$ stretch consistent with $NH_{hydrazinic}$ deprotonation. Thus, the mentioned solids were reacted with bis(diphenylphosphino)methane (dppm) and 1,1-bis(diphenylphosphino)ethylene (vdpp) to give **3a**, **3b**, and **4**, as appropriate (see the Experimental Section). In previous work,[22] we showed that the phosphine (PCP) angle in the bimetallic Pd/K compound was 116°, a value intermediate between the PCP angle for dppm and vdpp, of 109.5 and 120°, respectively. We anticipated that the greater flexibility of the $PC(sp^3)P$ angle in dppm as opposed to the more rigid $PC(sp^2)P$ angle in vdpp may hinder the appropriate arrangement of the ether rings needed for entrapping the potassium cation in the latter case. To shed further light on this issue, we treated **2a** and **2b**, independently, with the mentioned phosphanes. The reaction of the product labeled as **2a** with dppm (Scheme 1, via i) gave a mixture of **3a** and **3b**. The $^{31}P\{^1H\}$ NMR spectrum showed two singlets at 10.20 ppm and at 30.91 ppm that were assigned to the open disposition, **3b**, and the sandwiched, **3a**, species, respectively, in ca. 15:85 ratio; attempts to fully separate both compounds were unsuccessful, however, as crystals of the new sought for complex could be

https://doi.org/10.1021/acsomega.2c03526
ACS Omega 2022, 7, 37256−37263

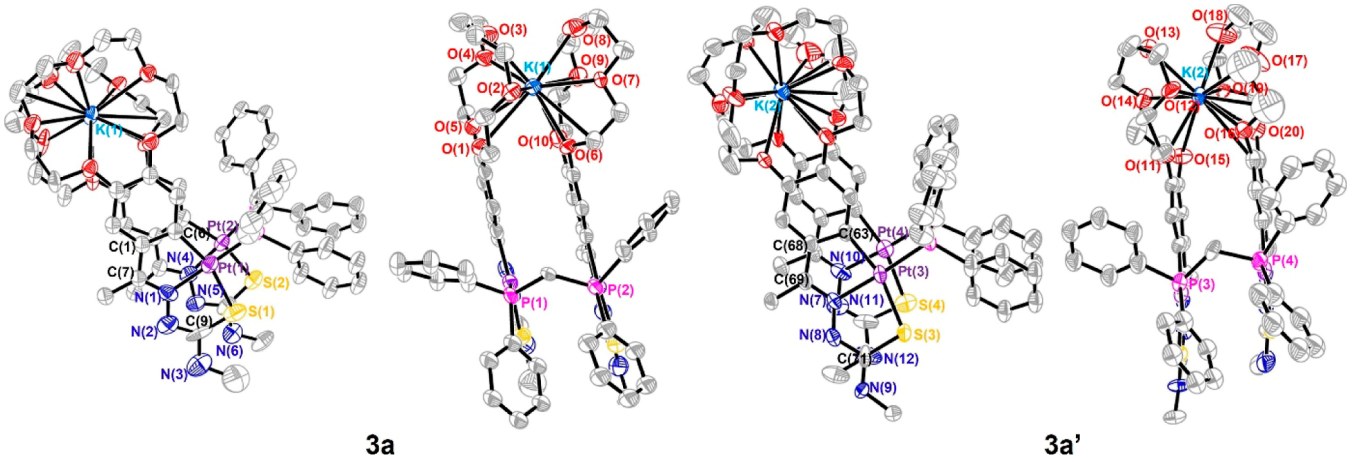

Figure 1. Thermal ellipsoid plot of **3** shown at the 30% probability level. Hydrogen atoms and minor disorder components have been omitted for clarity. Selected bond lengths (Å): Pt(1)−N(1) 2.008(14); Pt(1)−C(6) 2.030(14); Pt(1)−P(1) 2.235(4); Pt(1)−S(1) 2.333(4); Pt(2)−N(4) 1.952(14); Pt(2)−C(20) 2.041(14); Pt(2)−P(2) 2.221(5); Pt(2)−S(2) 2.348(4); Pt(3)−N(7) 2.010(10); Pt(3)−C(63) 2.036(15); Pt(3)−P(3) 2.231(3); Pt(3)−S(3) 2.363(4); Pt(4)−N(10) 2.021(11); Pt(4)−C(81) 2.049(16); Pt(4)−P(4) 2.224(4); Pt(4)−S(4) 2.336(5).

obtained, no further work was done regarding this issue. On the other hand, the reaction of the product labeled **2b** (lacking K^+ in the starting platinum salt) with dppm (Scheme 1, via ii) gave only **3b**, as confirmed by the $^{31}P\{^1H\}$ NMR spectrum that showed only a singlet resonance at 10.20 ppm; this reactivity trend parallels that for the palladium analogues;[22] the ^1H and $^{13}C\{^1H\}$ NMR data are quite in agreement with this arrangement. However, treatment of **1** with $PtCl_2(DMSO)_2$ and subsequently with vdpp gave, after work up, red solids for which the $^{31}P\{^1H\}$ NMR spectra were identical in all cases, displaying a singlet resonance at 33.64 ppm, leading us to conclude that the outcome of the reaction was the extended structure, **4**, regardless of the starting platinacycle. The ^1H NMR spectra showed absence of the H6 resonance after metalation of the phenyl ring, as well as shift of the H5, H2, Ha, and Hb resonances to higher field due to the shielding effect of the diphosphane phenyl rings. Additionally, the H5 signal showed satellites from coupling to the platinum nucleus, ^3J(HPt) 51.6 Hz.

Crystal Structure of Compound 3a. Single crystals of compound **3a** were obtained from an acetone solution of the **3a**/**3b** mixture in acetone. The presence of twins was successfully complete. In a similar manner to the sandwiched structured with palladium,[22] compound **3a** crystalizes in the triclinic system, space group $P\bar{1}$. The asymmetric unit contains two molecules of the compound (**3a** and **3a′**) which differ in the arrangement of the substituents on the NHMe group of the ligand (Figure 1). In addition, this asymmetric unit contains two chloride anions as counterions and 10 molecules of disordered solvent. Finally, the unit cell is formed by two asymmetric units between which no interaction is observed (Figure S3, Supporting Information).

The platinum atom is in a square-planar coordination environment with deviation from the mean plane between 0.010 and 0.068 Å and with rms close to zero in all cases. The bond distances and bond angles are within the expected values for compounds previously reported.[38] Except for the longer than expected Pt(1)−N(1), Pt(2)−N(4), Pt(3)−N(7), and Pt(4)−N(10) bond distances due to the trans influence of the phosphane ligand. The PCP angles are 116.26° (**3a**) and 117.58° (**3a′**), and the sum of angles at platinum is 360° in all cases, with the angles involving the phosphorus atom wider by ca. 10°, than those pertaining to the metallacycle and to the coordination rings. Moreover, the N(2)C(9)S(1) (**3a**) angle of the thiosemicarbazone is 129.01°, which is to the best of our knowledge and after checking the Cambridge Data Base, the largest value found for similar structures over the CCDC. The metallacycle units are present at angle ca. 1.52 and 4.29°, for **3a** and **3a′**, respectively, and the planes containing the crown ether oxygen atoms at angles of ca. 5.36 and 5.61°, for **3a** and **3a′** also, respectively, putting forward the nearly parallel arrangement of both cyclometallated moieties; even more so than that in the previously reported structure.[22] The distances between the centroids of the rings at platinum, phenyl, metallacycle, and coordination rings gave values between 3.47 and 3.71 Å (see the Supporting Information), and the angles between centroids and the normal to the plane of the rings gave values ca. 17.12−26.70°. These data are in agreement with the presence of slipping $\pi-\pi$ stacking interactions that contribute to increasing the stability of the molecule.[39]

Crystal Structure of 4. Suitable crystals were grown from a chloroform solution of **4**, although twined resolution proceeded smoothly (Figure 2). The compound crystallizes in the monoclinic system, space group $P2/c$. The asymmetric unit consists of one-half molecule, that is, the structure is crystallographically centrosymmetric with the inversion center situated at the C(31) atom between the two phosphorus atoms. The platinum atom is in a slightly distorted square-planar coordination environment bonded to four different atoms (C, N, S, and P), with deviation of the platinum atom ca. 0.163 Å from the mean coordination plane. All bond lengths and angles are within the expected values, with allowance for lengthening of the Pd(1)−N(1) bond, 2.053(2) Å, due to the trans influence of the phosphane ligand. The PCP angle is somewhat greater than that expected for a C(sp^2) carbon, 123.49° versus 120°, probably due to crystal packing. In this case, the difference between the angles involving the phosphorus atom and those inside the rings at platinum is not as pronounced as in the case of compound **3a**. Although the ancillary ligand is not the same, we presume that this difference in the angles involving the phosphorus atom is due to the lower stiffness of the open bridge structure compared to the sandwich structure. After examining the packing, it is possible to appreciate the dispositions of the crown ether moieties from

https://doi.org/10.1021/acsomega.2c03526
ACS Omega 2022, 7, 37256−37263

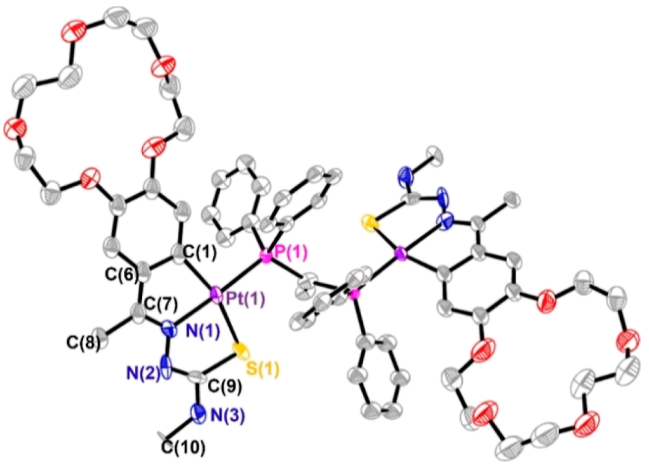

Figure 2. Thermal ellipsoid plot of **4** shown at the 30% probability. Hydrogen atoms and minor disorder components have been omitted for clarity. Selected bond lengths (Å) and angles (°): Pt(1)−N(1) 2.016(10); Pt(1)−C(2) 2.053(13); Pt(1)−P(1) 2.230(3); Pt(1)−S(1) 2.344(4); N(1)−Pt(1)−C(6) 79.2(5); N(1)−Pt(1)−P(1) 176.8(3); C(6)−Pt(1)−P(1) 97.6(4); N(1)−Pt(1)−S(1) 84.2(3); C(6)−Pt(1)−S(1) 163.1(4); P(1)−Pt(1)−S(1) 98.81(12); C(31)−P(1)−Pt(1) 113.33(18); C(9)−S(1)−Pt(1) 93.0(5); C(7)−N(1)−Pt(1) 118.2(9); N(2)−N(1)−Pt(1) 122.1(8).

different molecules facing each other displaying hydrogen bonds that probably stabilize the open conformation and oppose cation encapsulation (Figure S6, Supporting Information). Finally, it is worth mentioning that the cyclometallated part is arranged on opposite sides, which is the common disposition in this kind of structures.

DFT Calculations. To clarify the mechanism of potassium encapsulation, we sought to perform DFT calculations using Gaussian software,[40] on the assumption that encapsulation may be favored by dppm as it is more flexible than vdpp. The first approach was to study the influence of the phosphane in the stabilization of the closed or the open conformations for which five possible scenarios were evaluated using the crystallographic structures as starting points (Figure 4). Thus, the formation of a sandwich-type structure either both in the presence (labelled AK) or absence (A) of cations, the open structure with (BK) and without (B) cation coordination, and finally, the extended structure with one K^+ in each of the crown ether rings (BKK) were proposed (see the Supporting Information). This study separately deals with the two main effects that can stabilize the structures found, namely, the intramolecular interactions between the cyclometallated moieties and the influence of the coordination to the potassium cation. The structures were optimized using B3LYP[41]-D3[42] at the LANL2DZ[43]-ECP-6.31G(d)[44] level. Hessian calculations were performed to confirm the stationary points. Single-point calculations were performed for the optimized structures at the LANL2DZ-ECP-6.311++G**. The effect of the solvent was considered using the SMD[45] model with acetone as the solvent.

The thermodynamic cycle (Figure 3) used to link the free energy in solution and gas phase considers the free energies of solvation of the different components of the mixture, whereas the free energy of the complexation process or the conformational changes considers the difference in the free energy of each component (Table 1).

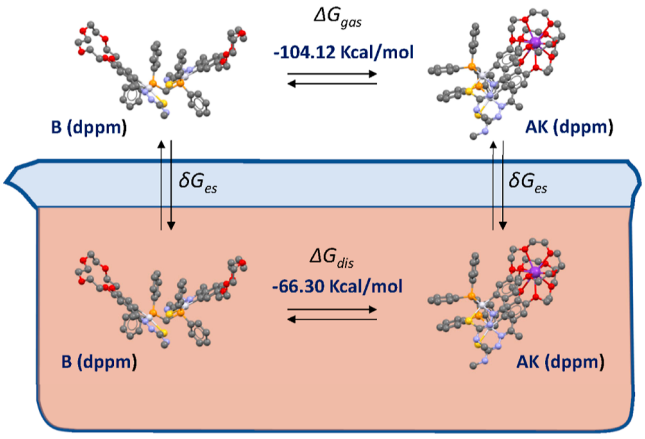

Figure 3. Schematic representation of the thermodynamic cycle used for the DFT calculations; free potassium ions are omitted for clarity.

The results show that the preferred conformer in the absence of cations is the sandwich arrangement, that is, structure **A** is more stable than **B** (Figure 4), both for the dppm complex, 5.90 and 7.15 Kcal/mol, ΔG_{sol} and ΔG_{gas}, respectively, as well as for the vdpp one, 7.57 and 9.86 Kcal/mol, ΔG_{sol} and ΔG_{gas}, also respectively (Table 1, entry 3). The coordination of the potassium ion in a sandwich fashion induces a stabilization in solution and in the gas phase in both cases, **A** → **AK** and **B** → **AK**, and the magnitude of this stabilization is fairly the same (Table 1, entries 1 and 2). It is worth mentioning here that this potassium encapsulation is so favorable that it also drives the closing of the open structure, **BK** → **AK** (Table 1, entry 4, values of ΔG_{dis} of −35.93 and −28.65 Kcal/mol for dppm and vdpp, respectively). The crystal obtained in the elongated conformation may be due to a stabilization caused by the intermolecular interactions with neighboring molecules, as suggested once simulated the packaging in the structure of **4** (Figure S6, Supporting Information).

Coordination of a single cation to the open disposition (BK) gives a variation of the free energy that is roughly half the variation of the formation of the sandwich coordination, and the addition of a second cation (BKK) does not stabilize the structure further than the sandwich situation. Using the values found for the complexation, the stability constants can be calculated (Table 2), showing lower values for the vdpp compound.

The calculated theoretical data could not be compared with the experimental data; however, the present framework has been used in the past to study similar compounds, and the discrepancies found for the gas phase and solution energies have been previously explained.[46,47] A source of error that could be of interest is the solution energy of the potassium cation in acetone, but to the best of our knowledge, this value has not been found due to the poor solubility of potassium salts in this solvent. Thus, the DFT calculations show that both compounds should be able to coordinate potassium cations, provided the latter can be present in the acetone solution; the dppm one showing a greater stability constant.

To shed further light on this issue, a simple experiment was carried out, based on the difference in ^{31}P NMR $\{^1H\}$ resonances for the sandwich and open structures for the dppm compounds, in the hope that it could be extrapolated to the vdpp case as proof of potassium coordination. Accordingly, a

https://doi.org/10.1021/acsomega.2c03526
ACS Omega 2022, 7, 37256−37263

Table 1. Calculated ΔG (Kcal/mol) for the Different Transformations between the Assumed Structures at 298 K

dppm	ΔG_{dis}	ΔG_{gas}	vdpp	ΔG_{dis}	ΔG_{gas}
A → AK	−60.40	−96.97	A → AK	−53.62	−85.72
B → AK	−66.30	−104.12	B → AK	−61.19	−95.58
A → B	5.90	7.15	A → B	7.57	9.86
BK → AK	−35.93	−46.44	BK → AK	−28.65	−38.77
AK → BKK	6.97	8.40	AK → BKK	0.43	0.33
BK → BKK	−28.96	−38.04	BK → BKK	−28.22	−38.43
B → BKK	−59.33	−95.72	B → BKK	−60.76	−95.25

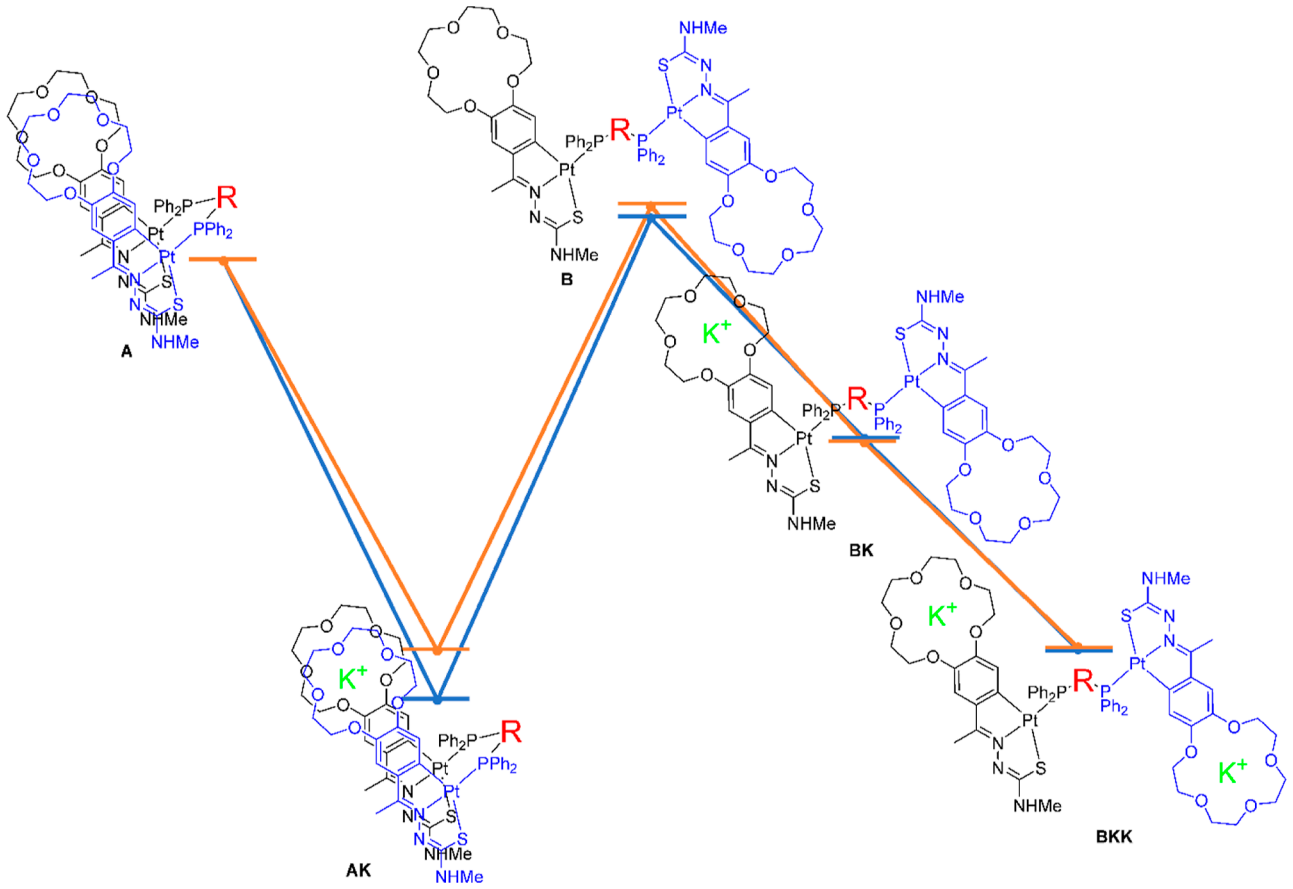

Figure 4. Relative energies of the different situations, taking into account the free cations as needed. The main differences can be observed in the sandwich form, where the dppm compound (blue) shows a lower energy, and in the open structure, where the vdpp (orange) shows a higher energy.

Table 2. Calculated Stability Constants for of the Complexes with a K^+ Coordinated in the Sandwich Mode

dppm	log K_{dis}	log K_{gas}	vdpp	log K_{dis}	log K_{gas}
A → AK	44.27	71.08	A → AK	39.31	62.84

small amount of the compound bearing the bridging vdpp phosphane was dissolved in a saturated solution of potassium nitrate in acetonitrile and the solution subjected to sonication action for 1 h, left to stand for a further 4 h, and then, the solvent was removed. The resulting orange-red residue was redissolved in deuterated acetone, and the ensuing ^{31}P NMR $\{^1H\}$ spectrum showed a shift to higher field of the phosphorus resonance, ca. 6 ppm, with respect to the spectrum of the parent compound **4**. In the absence of appropriate crystal structural analysis, we believe that this may be indicative of an incipient coordination of the potassium cation which could lead to a sandwich solution. Further experiments are currently underway in order to clarify this process.

EXPERIMENTAL SECTION

X-ray Structure Determination. Crystallographic data of the structures described in this work were collected on a Bruker Kappa Apex II diffractometer (Mo Kα radiation, λ = 0.71073 Å) equipped with a graphite monochromator by the method of the ω and φ scans at 293 K, integrated and corrected for absorption and solved and refined using routine techniques. All non-hydrogen atoms were refined anisotropically; hydrogen atoms were included in calculated positions and refined in the riding mode.

General Procedures. Solvents were used without previous purification. Chemicals were of reagent grade. The diphosphanes $Ph_2PCH_2PPh_2$ (dppm) and $PH_2PC(=CH_2)PPh_2$ (vdpp) were purchased from Sigma-Aldrich. Elemental

https://doi.org/10.1021/acsomega.2c03526
ACS Omega 2022, 7, 37256−37263

analyses were carried out on a thermo Finnigan, model flash 1112. Ir spectra were recorded with a Jasco FT/IR-4600 spectrometer equipped with an ATR, model ATR-PRO ONE. ^{1}H NMR spectra in solution were recorded in $CDCl_3$ or acetone-d_6 at room temperature on an Varian Inova 400 spectrometer. ^{13}C NMR {^{1}H} spectra were recorded at 100 MHz on a Bruker AMX 400 spectrometer. ^{31}P NMR {^{1}H} spectra were recorded at 162 MHz on a Bruker AMX 400 spectrometer. All chemical shifts are reported downfield from standards, TMS using the solvent signal ($CDCl_3$, δ ^{1}H = 7.26 ppm and acetone-d_6 δ^{1}H = 2.09) as reference and for ^{31}P relative to external H_3PO_4 (85%). All the NMR experiments were carried out using 5 mm o.d. tubes. The ESI mass spectra were recorded using a QSTAR Elite mass spectrometer, using acetonitrile or dichloromethane/ethanol as solvents. Potassium was determined by flame atomic emission spectrometry (PerkinElmer 3110 spectrometer) using the 766.5 nm emission wavelength (slit of 0.4 nm). The samples were digested with HNO_3/H_2O_2; the potassium standards were purchased from Scharlau. 4′-acetylbenzo-15-crown-5-ether thiosemicarbazone (**1**) has been synthetized following the literature.[22]

Synthesis of [K−[Pt{3,4-($C_8H_{16}O_5$)C_6H_3C(Me)=NN=C(S)-NHMe}]$_2$dppm]Cl ***3a*** *Via i.* Ethanol (20 cm^3) was added to a stirred solution of potassium tetrachloroplatinate (37.3 mg, 0.09 mmol) in water (3 cm^3). The solution was treated with 3,4-($C_8H_{16}O_5$)C_6H_3C(Me)=NN(H)C(=S)NHMe, **1** (40.0 mg, 0.10 mmol) and stirred for 24 h at 30 °C. The brown precipitate (**2a**) was filtered off, washed with water, dried, and added in acetone (10 cm^3). To the resulting suspension, the diphosphane dppm (319.34 mg, 0.101 mmol) was added (based on **1**), and the mixture was stirred for 24 h at 50 °C. Then, the solvent was removed under vacuum, and the product was recrystallized from dichloromethane/*n*-hexane. Yield 45.6 mg, 65% (based on **1**). (assuming 85:15 **3a**/**3b** ratio, see the text). ^{1}H NMR (400 MHz, acetone-d_6): 7.98 (m, 4H, *m*-Ph), 7.70 (m, 6H, *p*-Ph, *o*-Ph), 6.75 (s, 1H, H2), 5.91 (s, 1H, H5), 4.04 (m, 2H, Ha′), 3.79 (m, 2H, Hb′), 3.62 (m, 8H, Hc), 3.50 (m, 2H, Hb), 3.20 (m, 2H, Hb), 3.17 (d, 3H, NHMe, ^{3}J(NHMe) = 4.5 Hz), 3.04 (m, 2H, PCH_2P), 2.83 (s, 3H, MeC=N). ^{31}P{^{1}H} NMR (162 MHz, acetone-d_6): δ 30.91 (s, 1P, dppm). IR cm^{-1}: 3325 ϒ(N−H), 1517 υ(C=N). Anal. Found: C, 44.5; H, 4.3; N, 5.0; S, 3.9; K, 2.3% $C_{61}H_{72}ClKN_6O_{10}P_2Pt_2S_2$ (1640.06 g/mol) requires C, 44.7; H, 4.4; N, 5.1; S, 3.9; K, 2.4%. **3b** ^{31}P NMR {^{1}H} (162 MHz, acetone-d_6): δ 10.20 (s, 2P, dppm).

Synthesis of [Pt{3,4-($C_8H_{16}O_5$)C_6H_3C(Me)=NN=C(S)-NHMe}]$_2$dppm] ***3b*** *via ii.* 3,4-($C_8H_{16}O_5$)C_6H_3C(Me)=NN-(H)C(=S)−NHMe, **1** (51.5 mg, 0.13 mmol) was added to a solution of $PtCl_2(DMSO)_2$ (49.7 mg, 0.11 mmol) in methanol (20 cm^3). The resulting mixture was stirred for 1 h under reflux. Then, the reaction was cooled to 30 °C, and NaAcO (11.1 mg, 0.13 mmol) was added. The mixture was stirred for further 24 h at 30 °C, after which the solvent was removed, the residue (**2b**) was washed with water, dried, and added in acetone (10 cm^3). To the resulting suspension, the diphosphane dppm (38.68 mg, 0.101 mmol) was added (based on **1**), and the mixture was stirred for 24 h at 50 °C. Then, the solvent was removed under vacuum, and the product was recrystallized from dichloromethane/n-hexane. Yield 74.04 mg, 73% (based on **1**). ^{1}H NMR (400 MHz, acetone-d_6): 7.85 (m, 4H, *m*-Ph), 7.71 (m, 6H, *p*-Ph, *o*-Ph), 6.71 (s, 1H, H2), 5.86 (d, 1H, H5), 4.09 (m, 2H, Ha′), 3.67 (m, 2H, Hb′), 3.55 (m, 8H, Hc), 3.43 (m, 2H, Hb), 3.15 (m, 2H, Hb), 3.17 (d, 3H, NHMe, ^{3}J(NHMe) = 4.3 Hz, 3.1 (m, 2H, PCH_2P), 2.80 (s, 3H, MeC=N). ^{13}C{^{1}H} NMR (100 MHz, acetone-d_6): 158.4 (C=S), 159.5 (C=N), 143.7 (C1), 142.6 (C2), 117.2 (C3), 149.1 (C4), 149.5 (C5), 115 (C6), 71−68 (CH_2), 34.7 (PCH_2P) 29.1 (NHMe), 15.8 (Me), 14.93. ^{31}P{^{1}H} NMR (162 MHz, acetone-d_6): δ 10.20 (s, 2P, dppm). IR cm^{-1}: 3321 υ(N−H), 1520 υ(C=N). Anal. Found: C, 46.5; H, 4.4; N, 5.2; S, 4.0% $C_{61}H_{72}N_6O_{10}P_2Pt_2S_2$ (1565.6 g/mol) requires C, 46.8; H, 4.6; N, 5.4; S, 4.1%. ESI−MS *m*/*z*: = 1564 [{LH)Pt}$_2$(dppm)]$^+$.

Synthesis of [[Pt{3,4-($C_8H_{16}O_5$)C_6H_3C(Me)=NN=C(S)-NHMe}]$_2$vdpp] ***4.*** Compound **4** was prepared in a similar fashion from 3,4-($C_8H_{16}O_5$)C_6H_3C(Me)=NN−(H)C(=S)NHMe, **1** (40 mg, 0.10 mmol) and $PtCl_2(DMSO)_2$ (46.45 mg, 0.11 mmol). Yield 43.0 mg, 54% (based on **1**). ^{1}H NMR (400 MHz, acetone-d_6): δ 7.86 (m, 4H, *m*-Ph), 7.60 (m, 2H, *p*-Ph), 7.38 (m, 4H, *o*-Ph), 6.62 (d, 1H, H2), 6.21 (m, 1H, C=CH_2), 5.66 (d, 1H, H5, ^{4}J(H2P) = 2.0 Hz), 4.02 (m, 2H, Ha′), 3.81 (m, 2H, Hb′), 3.66 (m, 8H, Hc), 3.58 (m, 2H, Hb), 3.42 (m, 2H, Ha), 3.13 (d, 3H, NHMe, ^{3}J(NHMe) = 4.8 Hz), 2.61 (d, 3H, MeC=N). ^{13}C{^{1}H} NMR (100 MHz, acetone-d_6): 159.7 (C=S), 158.5 (C=N), 144.1 (C1), 142.0 (C2), 116.9 (C3), 149.2 (C4), 149.8 (C5), 128.1 (PC(=CH_2)P), 116 (C6), 110.3 (PC(=CH_2)P), 70−68 (CH_2), 29.1 (NHMe), 15.8 (Me), 14.93. ^{31}P{^{1}H} NMR (162 MHz, acetone-d_6): δ 33.64 (s, 2P, vdpp). IR cm^{-1}: 2866 υ(N−H), 1517 υ(C=N). Anal. Found: C, 47.2; H, 4.6; N, 5.2; S, 4.1%; $C_{62}H_{73}N_6O_{10}P_2Pt_2S_2$ (1578.53 g/mol) requires C, 47.2; H, 4.7; N, 5.3; S, 4.1%. ESI−MS *m*/*z*: = 1577 [{(LH)-Pt}$_2$(vdpp)]$^+$.

CONCLUSIONS

In conclusion, we have expanded the chemistry related to the synthesis of dinuclear phosphane-bridged thiosemicarbazone metallacycles containing 15-crown-5 ether rings capable of coordinating the K^+ cation in a sandwich mode between the two ether rings, extending its reproducibility to other metals, in particular platinum. In addition, experiments with the diphosphanes dppm and vdpp have been carried out to evaluate the effect of the ancillary ligand in the formation of the desired structure. It seems likely that the lower rigidity of dppm as opposed to vdpp allows for the formation of the sandwich potassium species with potassium in the former case. To better understand this process, DFT calculations were performed. From a thermodynamical point of view, compounds with both diphosphanes should present affinity toward the cation and coordinate it effectively, although the situation is somewhat more favorable for those with dppm; suggesting that choice of the diphosphane could influence the outcome. Also, the presence of potassium or of other cations in the media prior to the formation of the cyclometallated compounds must be avoided in order to obtain the open structures needed for further reaction as these cations will trigger the formation of sandwich coordinated species. Further studies concerning these issues are currently underway.

ASSOCIATED CONTENT

Supporting Information

The Supporting Information is available free of charge at https://pubs.acs.org/doi/10.1021/acsomega.2c03526.

https://doi.org/10.1021/acsomega.2c03526
ACS Omega 2022, 7, 37256−37263

DFT calculation results: optimized structures in solution and thermodynamic values for the compounds in the optimized conformations (PDF)

Crystal data and selected bond angle and bond length for **3a** (CIF)

Crystal data and selected bond angle and bond length for **4** (CIF)

AUTHOR INFORMATION

Corresponding Authors

Fátima Lucio-Martínez − *Department of Inorganic Chemistry, University of Santiago de Compostela, Santiago de Compostela E-15782, Spain*; Email: fatimaluciomartinez@gmail.com

José M. Vila − *Department of Inorganic Chemistry, University of Santiago de Compostela, Santiago de Compostela E-15782, Spain*; orcid.org/0000-0003-2196-1022; Email: josemanuel.vila@usc.es

Authors

Francisco Reigosa − *Department of Inorganic Chemistry, University of Santiago de Compostela, Santiago de Compostela E-15782, Spain*

Brais Bermúdez − *Department of Inorganic Chemistry, University of Santiago de Compostela, Santiago de Compostela E-15782, Spain*

Harry Adams − *Department of Chemistry, The University of Sheffield, Sheffield S3 7HF, U.K.*

M. Teresa Pereira − *Department of Inorganic Chemistry, University of Santiago de Compostela, Santiago de Compostela E-15782, Spain*

Complete contact information is available at: https://pubs.acs.org/10.1021/acsomega.2c03526

Notes

The authors declare no competing financial interest.

ACKNOWLEDGMENTS

This work was made possible, thanks to the financial support received from the Xunta de Galica (Galicia, Spain) under the Grupos de Referencia Competitiva Programme (Project GRC2015/009). F.L.-M. and F.R. thank the Spanish Ministry of Education (grants FPU13/05014 and FPU15/07145). We wish to thank Professor Alberto Fernández (UDC, Spain) for helpful discussions concerning X-ray data.

REFERENCES

(1) Jarolímová, Z.; Vishe, M.; Lacour, J.; Bakker, E. Potassium Ion-Selective Fluorescent and PH Independent Nanosensors Based on Functionalized Polyether Macrocycles. *Chem. Sci.* **2016**, *7*, 525−533.

(2) Qiu, J.; Zhang, Y.; Dong, C.; Huang, Y.; Sun, L.; Ruan, H.; Wang, H.; Li, X.; Wu, A. Rapid Colorimetric Detection of Potassium Ions Based on Crown Ether Modified Au NPs Sensor. *Sens. Actuators, B* **2019**, *281*, 783−788.

(3) Móczár, I.; Huszthy, P. Optically Active Crown Ether-Based Fluorescent Sensor Molecules: A Mini-Review. *Chirality* **2019**, *31*, 97−109.

(4) Liang, Y.; Wang, X.; Zhao, S.; He, P.; Luo, T.; Jiang, J.; Liang, W.; Cai, J.; Xu, H. A New Photoresponsive Bis (Crown Ether) for Extraction of Metal Ions. *ChemistrySelect* **2019**, *4*, 10316−10319.

(5) Ooi, T.; Maruoka, K. Recent Advances in Asymmetric Phase-Transfer Catalysis. *Angew. Chem., Int. Ed.* **2007**, *46*, 4222−4266.

(6) Kralj, M.; Tušek-Božić, L.; Frkanec, L. Biomedical Potentials of Crown Ethers: Prospective Antitumor Agents. *ChemMedChem* **2008**, *3*, 1478−1492.

(7) Herschede, S. R.; Gneid, H.; Dent, T.; Jaeger, E. B.; Lawson, L. B.; Busschaert, N. Bactericidal Urea Crown Ethers Target Phosphatidylethanolamine Membrane Lipids. *Org. Biomol. Chem.* **2021**, *19*, 3838−3843.

(8) Merzlyakova, E.; Wolf, S.; Lebedkin, S.; Bayarjargal, L.; Neumeier, B. L.; Bartenbach, D.; Holzer, C.; Klopper, W.; Winkler, B.; Kappes, M.; Feldmann, C. 18-Crown-6 Coordinated Metal Halides with Bright Luminescence and Nonlinear Optical Effects. *J. Am. Chem. Soc.* **2021**, *143*, 798−804.

(9) Park, J.; Kim, K. Y.; Kim, C.; Lee, J. H.; Kim, J. H.; Lee, S. S.; Choi, Y.; Jung, J. H. A Crown-Ether-Based Moldable Supramolecular Gel with Unusual Mechanical Properties and Controllable Electrical Conductivity Prepared by Cation-Mediated Cross-Linking. *Polym. Chem.* **2018**, *9*, 3900−3907.

(10) Leung, F. C. M.; Yam, V. W. W. Cation- and Solvent-Induced Supramolecular Aggregation Studies of Crown Ether-Containing Dinuclear Alkynylgold(I) Isocyanide Complexes. *Eur. J. Inorg. Chem.* **2017**, *2017*, 5271−5278.

(11) Yan, F.; Chen, F.; Wu, X. H.; Luo, J.; Zhou, X. S.; Horsley, J. R.; Abell, A. D.; Yu, J.; Jin, S.; Mao, B. W. Unique Metal Cation Recognition via Crown Ether-Derivatized Oligo-(Phenyleneethynylene) Molecular Junction. *J. Phys. Chem. C* **2020**, *124*, 8496−8503.

(12) Berdnikova, D. V.; Aliyeu, T. M.; Delbaere, S.; Fedorov, Y. V.; Jonusauskas, G.; Novikov, V. V.; Pavlov, A. A.; Peregudov, A. S.; Shepel', N. E.; Zubkov, F. I.; Fedorova, O. A. Regio- and Stereoselective [2 + 2] Photocycloaddition in Ba^{2+} Templated Supramolecular Dimers of Styryl-Derivatized Aza-Heterocycles. *Dyes Pigm.* **2017**, *139*, 397−402.

(13) Kapdi, A.; Maiti, D. *Palladacycles: Catalysis and Beyond*; Elsevier, 2019.

(14) Jurgens, S.; Kuhn, F. E.; Casini, A. Cyclometalated Complexes of Platinum and Gold with Biological Properties: State-of-the-Art and Future Perspectives. *Curr. Med. Chem.* **2018**, *25*, 437−461.

(15) Reigosa-Chamorro, F.; Raposo, L. R.; Munín-Cruz, P.; Pereira, M. T.; Roma-Rodrigues, C.; Baptista, P. V.; Fernandes, A. R.; Vila, J. M. In Vitro and in Vivo Effect of Palladacycles: Targeting A2780 Ovarian Carcinoma Cells and Modulation of Angiogenesis. *Inorg. Chem.* **2021**, *60*, 3939−3951.

(16) Oliveira, C. G.; Romero-Canelón, I.; Coverdale, J. P. C.; Maia, P. I. S.; Clarkson, G. J.; Deflon, V. M.; Sadler, P. J. Novel Tetranuclear PdII and PtII anticancer Complexes Derived from Pyrene Thiosemicarbazones. *Dalton Trans.* **2020**, *49*, 9595−9604.

(17) Bezsoudnova, E. Y.; Ryabov, A. D. Water-Soluble Cyclopalladated Aryl Oxime: A Potent "green" Catalyst. *J. Organomet. Chem.* **2001**, *622*, 38−42.

(18) Castro-Juiz, S.; Fernández, A.; López-Torres, M.; Vázquez-García, D.; Suárez, A. J.; Vila, J. M.; Fernández, J. J. Crown Ether Palladacycles as Metalloligands: Suitable Precursors for Tetranuclear Mixed Transition/Non-Transition Metal Complexes. *Organometallics* **2009**, *28*, 6657−6665.

(19) Coco, S.; Cordovilla, C.; Espinet, P.; Gallani, J. L.; Guillon, D.; Donnio, B. Supramolecular Aggregates in Fluid Phases: Mesomorphic Ortho-Palladated Complexes with Substituted Crown Ethers and Their Potassium Adducts. *Eur. J. Inorg. Chem.* **2008**, *2008*, 1210−1218.

(20) Fernández, A.; López-Torres, M.; Castro-Juiz, S.; Merino, M.; Vázquez-García, D.; Vila, J. M.; Fernández, J. J. Dimetalated Crown Ether Schiff Base Palladacycles. Influence of the Carbon Chain Length on the Coordination Mode of Bidentate Phosphines. Crystal and Molecular Structure of the Novel Complex $[Pd_2\{1,4\text{-}[C(H)=N\{9,10\text{-}(C_8H_{16}O_5)C_6H_3\}]\ 2C_6H_2\text{-}2,C5\}(Cl)_2\{\mu\text{-}Ph_2P$. *Organometallics* **2011**, *30*, 386−395.

(21) Vázquez-García, D.; Fernández, A.; López-Torres, M.; Rodríguez, A.; Varela, A.; Pereira, M. T.; Vila, J. M.; Fernández, J. J. Functionalized Palladacycles with Crown Ether Rings Derived from

Terdentate [C, N, N] Ligands. Crystal and Molecular Structure of the Dinuclear Palladium/Silver Complex [Pd{3,4-($AgC_{10}H_{20}O_6$)-$C_6H_2C(Me)=NN(H)$ (4′-ClC $4H_2N_2$)}(PPh_3)][CF_3SO_3]$_2$. *Organometallics* **2011**, *30*, 396−404.

(22) Lucio-Martínez, F.; Bermúdez, B.; Ortigueira, J. M.; Adams, H.; Fernández, A.; Pereira, M. T.; Vila, J. M. A Highly Effective Strategy for Encapsulating Potassium Cations in Small Crown Ether Rings on a Dinuclear Palladium Complex. *Chem. - Eur. J.* **2017**, *23*, 6255−6258.

(23) Dietrich, B.; Viout, P.; Lehn, J.-M. *Macrocyclic Chemistry—Aspects of Organic and Inorganic Supramolecular Chemistry*; VHC: New York, 1993; p 174.

(24) Peters, J. C.; Odom, A. L.; Cummins, C. C. A terminal molybdenum carbide prepared by methylidyne deprotonation. *Chem. Commun.* **1997**, 1995−1996.

(25) Lin, C.-Y.; Fettinger, J. C.; Chilton, N. F.; Formanuik, A.; Grandjean, F.; Long, G. J.; Power, P. P. Salts of the two-coordinate homoleptic manganese(i) dialkyl anion [Mn{C(SiMe3)3}2]$^-$ with quenched orbital magnetism. *Chem. Commun.* **2015**, *51*, 13275−13278.

(26) King, D. M.; McMaster, J.; Tuna, F.; McInnes, E. J. L.; Lewis, W.; Blake, A. J.; Liddle, S. T. Synthesis and Characterization of an f-Block Terminal Parent Imido [U=NH] Complex: A Masked Uranium(IV) Nitride. *J. Am. Chem. Soc.* **2014**, *136*, 5619−5622.

(27) Liddle, S. T.; Clegg, W. Formation of [M(15-crown-5)2]2[Li(NHPy)3] (M=K or Cs): the first structurally authenticated examples of a monomeric lithium species coordinated by three amide anions. *J. Chem. Soc., Dalton Trans.* **2001**, *24*, 3549−3550.

(28) Gromov, S. P.; Vedernikov, A. I.; Lobova, N. A.; Kuz'mina, L. G.; Basok, S. S.; Strelenko, Y. A.; Alfimov, M. V.; Howard, J. A. K. Controlled self-assembly of bis(crown)stilbenes into unusual bis-sandwich complexes: structure and stereoselective [2+2] photocycloaddition. *New J. Chem.* **2011**, *35*, 724−737.

(29) Martínez, J.; Cabaleiro-Lago, E. M.; Ortigueira, J. M.; Pereira, M. T.; Frieiro, P.; Lucio, F.; Vila, J. M. Synthesis and reactivity of thiosemicarbazone palladacycles. Crystal structure analysis and theoretical calculations. *Inorg. Chim. Acta* **2016**, *449*, 20−30.

(30) Martínez, J.; Pereira, M. T.; Ortigueira, J. M.; Bermúdez, B.; Antelo, J. M.; Fernández, A.; Vila, J. M. Synthesis and structural characterization of tridentate [C,N,S] thiosemicarbazone palladacycles. Crystal and molecular structures of [Pd{3-$FC_6H_3C(Me)$-NNC(S)NHMe}]$_4$, [Pd{4-$FC_6H_3C(Me)$NNC(S)NHEt}]$_4$ and [($Pd\{2\text{-}BrC_6H_3C(Me)NNC(S)NHPh\}$)$_2$($\mu$-$Ph_2P(CH_2)_2PPh_2$)]. *Polyhedron* **2012**, *31*, 217−226.

(31) Antelo, J. M.; Adrio, L.; Pereira, M.; Ortigueira, J. M.; Fernández, J. J.; Vila, J. M. Synthesis and structural characterization of palladium and platinum bimetallic compounds derived from bidentate P, S-palladacycle metaloligands. *Cryst. Growth Des.* **2010**, *10*, 700−708.

(32) Adrio, L.; Antelo, J. M.; Fernández, J. J.; Hii, K. K.; Pereira, M. T.; Vila, J. M. [Pd{2-CH_2-5-$MeC_6H_3C(H)$=NN=C(S)NHEt}]$_3$: An unprecedented trinuclear cyclometallated palladium(II) cluster through induced flexibility in the metallated ring. *J. Organomet. Chem.* **2009**, *694*, 747−751.

(33) Lobana, T. S. Activation of C−H bonds of thiosemicarbazones by transition metals: Synthesis, structures and importance of cyclometallated compounds. *RSC Adv.* **2015**, *5*, 37231−37274.

(34) Lata, D.; Teresa Pereira, M.; Ortigueira, J. M.; Martínez, J.; Bermúdez, B.; Fernández, J. J.; Vila, J. M. Thiosemicarbazone platinacycles with tertiary phosphines. Preparation of novel heterodinuclear platinum-tungsten complexes. *Polyhedron* **2012**, *41*, 30−39.

(35) Antelo, J. M.; Adrio, L.; Pereira, M.; Ortigueira, J. M.; Fernández, J. J.; Vila, J. M. Synthesis and Structural Characterization of Palladium and Platinum Bimetallic Compounds Derived from Bidentate P, S-Palladacycle Metaloligands. *Cryst. Growth Des.* **2010**, *10*, 700−708.

(36) Vila, J. M.; Pereira, M. T.; Ortigueira, J. M.; Graña, M.; Lata, D.; Suárez, A.; Fernández, J. J.; Fernández, A.; López-Torres, M.; Adams, H. Formation, Characterization, and Structural Studies of Novel Thiosemicarbazone Palladium(II) Complexes. Crystal Structures of [{Pd[$C_6H_4C(Et)$=NN=C(S)NH_2]}$_4$], [Pd{$C_6H_4C(Et)$=NN= C(S)NH_2}($PMePh_2$)] and [{Pd[$C_6H_4C(Et$=NN=C(S)-NH_2]}2(μ-$Ph_2PCH_2PPh_2$)]. *J. Chem. Soc., Dalton Trans.* **1999**, *0*, 4193−4201.

(37) Bermúdez, B. Compuestos Ciclometalados de Paladio y Platino. Reacciones de Acoplamiento y Catálisis. Tesis Doctoral, Ph.D. Dissertation, Universidad de Santiago de Compostela, 2014.

(38) Vázquez-García, D.; Fernández, A.; López-Torres, M.; Rodríguez, A.; Gómez-Blanco, N.; Viader, C.; Vila, J. M.; Fernández, J. J. Reactivity of C(Sp^2)-Pd and C(Sp^3)-Pd Bonded Palladacycles with Diphosphines. Crystal and Molecular Structure of the Novel A-Frame Complex [{Pd[2,5-$Me_2C_6H_2C(H)N$(2,4,6-$Me_3C_6H_2$)-C6]}$_2$(μ-$Ph_2PCH_2PPh_2$)$_2$(μ-Cl)][PF_6]. *J. Organomet. Chem.* **2011**, *696*, 764−771.

(39) Pereira, M. T.; Antelo, J. M.; Adrio, L. A.; Martínez, J.; Ortigueira, J. M.; López-Torres, M.; Vila, J. M. Novel Bidentate [N, S] Palladacycle Metalloligands 1 H−15 N HMBC as a Decisive NMR Technique for the Structural Characterization of Palladium−Rhodium and Palladium−Palladium Bimetallic Complexes. *Organometallics* **2014**, *33*, 3265−3274.

(40) Frisch, M. J.; Trucks, G. W.; Schlegel, H. B.; Scuseria, G. E.; Robb, M. a.; Cheeseman, J. R.; Scalmani, G.; Barone, V.; Petersson, G. A.; Nakatsuji, H.; Li, X.; Caricato, M.; Marenich, a. V.; Bloino, J.; Janesko, B. G.; Gomperts, R.; Mennucci, B.; Hratchian, H. P.; Ortiz, J. V.; Izmaylov, a. F.; Sonnenberg, J. L.; Williams; Ding, F.; Lipparini, F.; Egidi, F.; Goings, J.; Peng, B.; Petrone, A.; Henderson, T.; Ranasinghe, D.; Zakrzewski, V. G.; Gao, J.; Rega, N.; Zheng, G.; Liang, W.; Hada, M.; Ehara, M.; Toyota, K.; Fukuda, R.; Hasegawa, J.; Ishida, M.; Nakajima, T.; Honda, Y.; Kitao, O.; Nakai, H.; Vreven, T.; Throssell, K.; Montgomery, J. a., Jr.; Peralta, J. E.; Ogliaro, F.; Bearpark, M. J.; Heyd, J. J.; Brothers, E. N.; Kudin, K. N.; Staroverov, V. N.; Keith, T. a.; Kobayashi, R.; Normand, J.; Raghavachari, K.; Rendell, a. P.; Burant, J. C.; Iyengar, S. S.; Tomasi, J.; Cossi, M.; Millam, J. M.; Klene, M.; Adamo, C.; Cammi, R.; Ochterski, J. W.; Martin, R. L.; Morokuma, K.; Farkas, O.; Foresman, J. B.; Fox, D. J. *Gaussian 16*, Revision C.01; Gaussian, Inc.: Wallin, 2016.

(41) Becke, A. D. Density-Functional Thermochemistry. III. The Role of Exact Exchange Hydrocarbons. *J. Chem. Phys.* **1993**, *98*, 5648.

(42) Grimme, S.; Antony, J.; Ehrlich, S.; Krieg, H. A Consistent and Accurate Ab Initio Parametrization of Density Functional Dispersion Correction (DFT-D) for the 94 Elements H-Pu. *J. Chem. Phys.* **2010**, *132*, 154104.

(43) Hay, P. J.; Wadt, W. R. Ab Initio Effective Core Potentials for Molecular Calculations. Potentials for the Transition Metal Atoms Sc to Hg. *J. Chem. Phys.* **1985**, *82*, 270−283.

(44) Ditchfield, R.; Hehre, W. J.; Pople, J. A. Self-Consistent Molecular-Orbital Methods. IX. An Extended Gaussian-Type Basis for Molecular-Orbital Studies of Organic Molecules. *J. Chem. Phys.* **1971**, *54*, 724−728.

(45) Marenich, A. V.; Cramer, C. J.; Truhlar, D. G. Universal Solvation Model Based on Solute Electron Density and on a Continuum Model of the Solvent Defined by the Bulk Dielectric Constant and Atomic Surface Tensions. *J. Phys. Chem. B* **2009**, *113*, 6378−6396.

(46) Achazi, A. J.; von Krbek, L. K. S.; Schalley, C. A.; Paulus, B. Theoretical and Experimental Investigation of Crown/Ammonium Complexes in Solution. *J. Comput. Chem.* **2015**, *37*, 18−24.

(47) Behjatmanesh-Ardakani, R. DFT-B3LYP and SMD Study on the Interactions between Aza-, Diaza-, and Triaza-12-Crown-4 (An-12-Crown-4, n = 1, 2, 3) with Na+ in the Gas Phase and Acetonitrile Solution. *Struct. Chem.* **2014**, *25*, 919−929.

https://doi.org/10.1021/acsomega.2c03526
ACS Omega 2022, 7, 37256−37263